TRENDS IN SCIENCES 2026; 23(3): 11471
https://doi.org/10.48048/tis.2026.11471 RESEARCH ARTICLE

Enhanced Conductive Polymer Sulfonated Polyeugenol-Graphene Oxide Composite for Eco-Friendly Supercapacitor Electrodes

Ngadiwiyana*, Andi Nugroho, Ismiyarto, Purbowatingrum Ria Sarjono, Damar Nurwahyu Bima and Irma Fifa Yanti

Department of Chemistry, Faculty of Science and Mathematics, Diponegoro University, Semarang 50275, Indonesia

(*Corresponding Author: ngadiwiyana@lecturer.undip.ac.id)

Received: 2 August 2025, Revised: 28 August 2025, Accepted: 1 October 2025, Published: 5 December 2025

Abstract

Conductive polymers derived from renewable resources have attracted increasing attention as environmentally friendly alternatives-based polymers such as polyaniline (PANI), polypyrrole (PPy), and polystyrene (PST) for supercapacitor electrode materials. Among them, polyeugenol represents a promising candidate due to its renewable origin and versatile functional groups. In this study, a composite of sulfonated eugenol–diallyl phthalate copolymer (SPEGDAF) and graphene oxide (GO) was synthesized and evaluated as a supercapacitor electrode material. The research encompassed several stages: Synthesis of the eugenol–diallyl phthalate copolymer (PEGDAF), sulfonation to yield SPEGDAF, synthesis of graphene oxide, fabrication of the SPEGDAF/GO composite, and subsequent electrochemical performance testing. Structural and thermal characterizations of PEGDAF and SPEGDAF were conducted using FTIR spectroscopy, TGA-DTG, and molecular weight analysis. Sulfonation introduced sulfonate groups, which raised the melting point from 84 - 110 °C and increased the molecular weight from 7,611.06 Da to 13,674.54 Da. The sulfonation degree was determined to be 31.16%, corresponding to a cation exchange capacity of 3.856 meq/g. FTIR and XRD analyses of the synthesized graphene oxide confirmed the presence of oxygen-containing functional groups and crystalline features. The incorporation of GO into SPEGDAF resulted in distinct FTIR spectral enhancements and notable improvements in electrochemical behavior. Cyclic voltammetry revealed a specific capacitance of 2.47 F/g, while electrochemical impedance spectroscopy indicated an ionic conductivity of 4.02×10^{-4} S/cm. These findings demonstrate that the integration of GO into SPEGDAF effectively enhances the charge storage and ionic transport properties of the composite. Overall, this study highlights the potential of polyeugenol-derived composites as sustainable for supercapacitor applications, underscoring their promise as renewable and environmentally responsible alternatives for future energy storage technologies.

Keywords: Polyeugenol, Sulfonation, Graphene oxide, Electrode, Supercapacitor

Introduction

Electrochemical capacitors or commonly known as supercapacitors, are devices that have great potential in power supply and recharging [1]. The potential of supercapacitors attracts attention because of their prominent advantages, such as significant power density, the ability to charge and discharge quickly, a wider operating temperature range, lower maintenance costs, the ability to be designed in small, lightweight, flexible sizes, and long cycle life [2]. In supercapacitors, electrodes play an important role in the energy storage mechanism. Materials employed as electrodes in supercapacitors consist of carbon-based substances, metal oxides, and electrically conductive polymers [3]. The use of conductive polymers as electrodes is more promising than other materials because conductive polymers have good electrical conductivity, low manufacturing costs, and high specific capacitance [4].

Conductive polymers that are often used in supercapasitors are polyaniline (PANI), polypyrrole (PPy), polythiophene (PTh), and sulfonated polystyrene (PST) [4]. These polymers are synthesized from petroleum and petrochemical-based materials, the

process of which can cause environmental problems such as global warming and the greenhouse effect [5]. The decline in petroleum reserves and the negative impacts on the environment encourage the development of alternatives based on renewable natural resources as a substitute for petroleum, especially in the polymer industry sector.

One of the natural and renewable polymers that can be used as a supercapacitor electrode material is polyeugenol. This is because polyeugenol is derived from clove oil, which is continuously available in nature and renewable, in contrast to PANI, PPy, PTh, and PST that originate from petroleum-based sources, the extraction and waste of which may cause environmental damage. The aromatic structure and active functional groups such as hydroxyl and methoxy enable polyeugenol to participate in electrochemical charge storage, making it a promising candidate for use as a sustainable electrode material [6]. However, one drawback of using polyeugenol as a supercapacitor electrode is the generation of heat during faradaic reactions that occur during charge storage and transfer, which can affect its thermal stability and performance [7]. The heat generated during operation can compromise the performance of polyeugenol as a supercapacitor electrode material [8]. To address this issue, modification through the introduction of cross-linking agents is essential to improve its thermal stability and overall durability. Diallyl phthalate is used as the cross-linking agent due to its ability to enhance thermal resistance, thereby improving the overall performance of the supercapacitor electrode material [7]. The performance of eugenol diallyl phthalate copolymer (PEGDAF) as a supercapacitor electrode material can be optimized by adding sulfonate groups (–SO_3H). The addition of this sulfonate group is expected to increase the cation exchange capacity, so that the electrical conductivity increases [9].

Polyeugenol contains a large number of hydroxyl groups (–OH), which provide the potential for application in composite materials, to increase their capacitance and conductivity as electrode materials in supercapacitors. The filler/reinforcement material that is often used in composites for supercapacitor materials is graphene oxide (GO). Graphene oxide is a derivative of graphene in the form of sheets with oxygen groups (−OH, −COOH, −CHO and epoxy groups) [10]. GO is a two-dimensional material with applications in various fields, such as membranes [11], ion separators [12], adsorbents [13], composites [14], and many others. GO has a large surface area, layered structure, high intercalation ability, superior mechanical properties, and good ion exchange ability [15]. These advantages make GO often found as a reinforcing material in composites. Compositing with GO is expected to increase the capacitance and electrical conductivity of supercapacitor electrode materials [16].

Previous research has analyzed the potential of sulfonated eugenol diallyl phthalate copolymers (SPEGDAF) as environmentally friendly materials for supercapacitor electrodes. Ngadiwiyana *et al*. [17] reported that SPEGDAF have specific capacitance and electrical conductivity capabilities that can be used as supercapacitor electrodes. It was demonstrated an increase in the material's conductivity before and after sulfonation, from 4.76×10^{-6} to 7.58×10^{-6} S/cm. Research by Li *et al*. [18] showed that the compositing of graphene oxide in polyaniline (PANI) showed an increase in specific capacitance and ion conductivity Composites with GO increased the capacitance of PANI material from 47.7 - 199.6 F/g. Research by Kianfar [19] coduncted the integration of graphene derivatives with organic materials such as polymers can enhance miniaturization, functionality, and overall material efficiency. Rattanaveeranon [20] also reported the integration material with graphene nanocomposites not only enhances performance but also aligns with green material innovation, offering a pathway toward more accessible and environmentally friendly energy storage solutions. In this study, SPEGDAF was synthesized and modified due to its renewable and environmentally friendly nature, while its performance as a supercapacitor electrode was enhanced through compositing with GO. This research is anticipated to contribute insights toward the development of high-performance and eco-friendly supercapacitors. Furthermore, it aims to enhance the functional value of eugenol and clove oil by promoting their optimal use as abundant and renewable natural resources in Indonesia.

Materials and methods

Chemicals and instrumentation

Chemicals used for polymer synthesis were eugenol ($C_{10}H_{12}O_2$, ≥ 98%, Merck, Germany), diallyl

phthalate ($C_{14}H_{14}O_4$, ≥ 97% purity, Merck, Germany), boron trifluoride etherate ($BF_3{-}O(C_2H_5)_2$, ≥ 98% purity, Merck, Germany), chloroform ($CHCl_3$, ≥ 99.8%, Merck, Germany), methanol (CH_3OH, ≥ 99.9%, Merck, Germany), ethanol (C_2H_5OH, 96%, Merck, Germany), dichloromethane (CH_2Cl_2, ≥ 99.9%, Merck, Germany), ethyl acetate ($C_4H_8O_2$, ≥ 99.5%, Merck, Germany), diethyl ether ($C_4H_{10}O$, ≥ 99.8%, Merck, Germany), and anhydrous sodium sulfate (Na_2SO_4, ≥ 99%, Merck, Germany). Chemicals used for sulfonation were sulfuric acid (H_2SO_4, 98%, Merck, Germany), sodium chloride (NaCl, ≥ 99.5%, Merck, Germany), sodium hydroxide (NaOH, ≥ 98%, Merck, Germany), and phenolphthalein indicator (PP indicator, analytical grade, Merck, Germany). Chemicals used for GO synthesis were distilled water, graphite powder (≥ 99%, Merck, Germany), hydrogen peroxide (H_2O_2, 30%, Merck, Germany), potassium permanganate ($KMnO_4$, ≥ 99%, Merck, Germany), hydrochloric acid (HCl, 37%, Merck, Germany), universal pH indicator, and filter paper. Chemicals used for electrode preparation were tetrahydrofuran (THF, ≥ 99.9%, Merck, Germany), acetone (C_3H_6O, ≥ 99.5%, Merck, Germany), sandpaper, copper plate (0.5×5 cm^2), and aluminum foil.

The instrumentation used were Fisher-John melting point apparatus, Ultrasonication, Cary 630 FTIR Spectrometer, Rodeostat (all from the U.S.A.). Powder X-ray Diffraction (P-XRD), Centrifuge (HETTICH), Thermogravimetric Analyzer (TG7300), (all from German), and PalmSens4 Electrochemical Impedance Analyser/Potentiostat/Galvanostat which were manufactured in Netherland.

Synthesis of eugenol diallyl phthalate copolymer (PEGDAF)

The procedure of synthesis PEGDAF was carried out based on the previous study conducted by Ngadiwiyana *et al*. [21]. Eugenol (65 mmol, 10.03 mL) and diallyl phthalate (6.5 mmol, 1.427 mL) were put into a three-necked flask that had been assembled in a reflux system with nitrogen gas (N_2) flow. $BF_3O(C_2H_5)_2$ (5 mL) was added slowly using a dropping funnel and then stirred for 24 h. Methanol (2 mL) was added to stop the polymerization reaction, and then the solution was left for 4 h. The solution formed thickened and changed color from yellow to blackish brown. The polymer formed was dissolved in diethyl ether (50 mL), then neutralized through a washing process using distilled water until it reached a neutral pH. The polymer solution in diethyl ether and the water layer were separated using a separating funnel. The remaining polymer dissolved in diethyl ether is evaporated in a desiccator and then ground in to powder.

Sulfonation eugenol diallyl phthalate copolymer (SPEGDAF)

The procedure of Sulfonation PEGDAF was carried out based on the on the previous study conducted by Ngadiwiyana *et al*. [21]. PEGDAF (4 g) was dissolved in chloroform (60 mL) in a three-necked flask. Sulfuric acid (0.03 mol, 1.6 mL) was added and then the solution was refluxed at 60 °C while being stirred for two hours with nitrogen gas (N_2) flowing. Cold distilled water (100 mL) was added until two layers were formed. The two layers were separated using a separating funnel. The layer containing the polymer was evaporated in a desiccator and then milled to obtain powder.

Synthesis of graphene oxide (GO)

GO was synthesized using a modified hummers method without $NaNO_3$ [22]. Graphite powder (4 g) was added with 98% sulfuric acid (100 mL) in a 1,000 mL beaker and the temperature was maintained below 10 °C while stirring. Potassium permanganate (12 g) was added slowly while maintaining the temperature below 10 °C. After that, distilled water (100 mL) was added dropwise while the temperature was raised to 90 °C. Distilled water (300 mL) and 30% hydrogen peroxide (20 mL) were added directly and the solution was left overnight at room temperature under ambient air conditions. The solution was filtered and the residue was washed with 10% HCl, then neutralized. The neutralized residue was dissolved in distilled water and ultrasonicated for 20 min. The graphene oxide was filtered and dried in an oven at 60 °C.

Synthesis of sulfonated eugenol diallyl phthalate copolymer/Graphene Oxide composite (SPEGDAF/GO)

SPEGDAF (0.9 g) was dissolved in THF (2.5 mL) in a vial bottle. The amount of THF was sufficient to fully dissolve the polymer under the described conditions. The dissolved SPEGDAF was then added with GO using a mass ratio (g) of 9:1. Only this ratio

was investigated in the present work. The mixture was stirred using a stirrer for 90 min, then ultrasonicated for 30 min and stirred again for 30 min.

Preparation of working electrode

The working electrode for electrochemical measurements was carried out by coating the PEGDAF, SPEGDAF, and SPEGDAF/GO composite on copper metal. Copper metal was prepared by polishing the copper plate (0.5×5 cm^2) with sandpaper. The plate was washed using distilled water, acetone, and then distilled water again in sequence. The copper metal plate was coated with a composite solution using the drop-casting method, followed by drying at room temperature overnight under ambient air conditions.

Electrochemical measurements

The electrochemical performance was evaluated using a three-electrode system, where PEGDAF, SPEGDAF, and SPEGDAF/GO composite functioned as the working electrodes. A platinum (Pt) plate served as the counter electrode, while Ag/AgCl was used as the reference electrode. An 1 M HCl solution was employed as the electrolyte. Cyclic voltammetry (CV) measurements were conducted using a rodeostat with a scan rate of 5 mV/s within a potential window from – 0.3 to + 0.1 V. Additionally, Electrochemical Impedance Spectroscopy (EIS) analysis was performed using a PalmSens4 Electrochemical Impedance Analyzer across a frequency range of 0.01 Hz to 10^5 Hz.

Results and discussion

Synthesis of eugenol diallyl phthalate copolymer (PEGDAF)

The synthesis of PEGDAF is carried out through a cationic addition polymerization reaction with boron trifluoride etherate as the initiator. The copolymerization process consists of initiation, propagation, and termination stages. In initiation, carbocation formation occurs as indicated by a color change from yellow to blackish red. In propagation, the monomer attacks the carbocation to form a new carbocation. Propagation continues to form longer polymer chain marked by phase change. Termination is the last stage of copolymerization where the copolymerization process is stopped by adding methanol and polymer changes to a solid. The copolymerization reaction mechanism is shown in **Figure 1**.

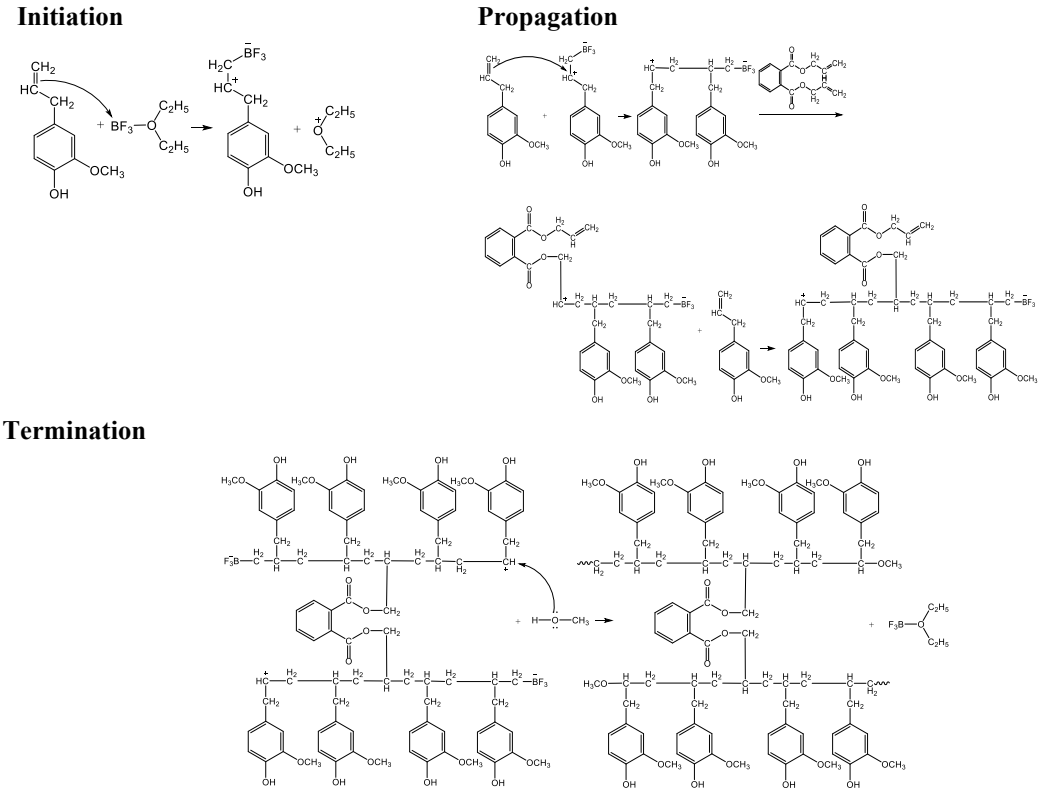

Figure 1 Reaction mechanism of synthesis PEGDAF.

The sythesized PEGDAF is a pink solid powder with a yield of 95.1%. Soluble in methanol, dichloromethane, ethyl acetate, chloroform, and insoluble in aquadest. PEGDAF has a melting point of 84 ºC and a molecular weight of 7,611.06 daltons. To confirm the success of the copolymerization process, functional group analysis was conducted using FTIR as shown in **Figure 2**. The success of copolymerization is indicated by the absence of C=C alkene absorption band (around 1,640 cm^{-1}) in PEGDAF. The loss of vinyl groups is due to the addition reaction in each monomer. The presence of C=O ester absorption band (around 1,721 cm^{-1}) from diallyl phthalate indicates that cross-linking has occurred. The presence of O−H absorption band (around 3,500 cm^{-1}) from eugenol signifying the successful synthesis of PEGDAF.

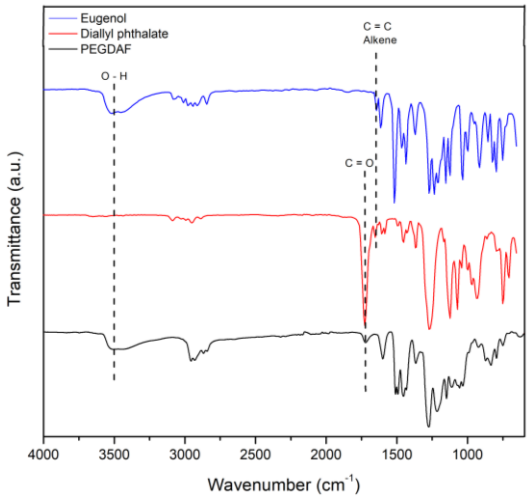

Figure 2 FTIR Spectra of PEGDAF.

The thermal stability of PEGDAF was evaluated using Thermogravimetric Analysis (TGA) and its derivative (DTG), as presented in **Figure 3**. The analysis showed that PEGDAF experienced mass losses of 5% and 10% at temperatures of 176 and 219 °C, respectively. These weight losses are attributed to the decomposition of side groups such as methyl (–CH_3) and methoxy (–OCH_3), which require relatively high temperatures to break their bonds. In comparison, polyeugenol exhibited 5% and 10% mass losses at lower temperatures, 75 and 186 °C, respectively, indicating a lower thermal resistance. The higher thermal stability of PEGDAF demonstrates that cross-linking polyeugenol with diallyl phthalate significantly enhances its thermal resistance. This improvement is particularly advantageous for applications involving faradaic processes, where materials are subjected to elevated temperatures and electrochemical stress.

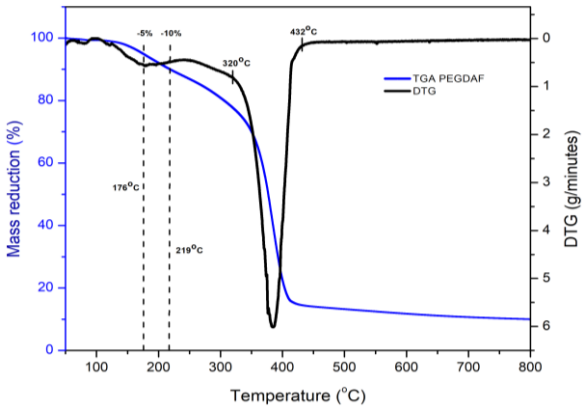

Figure 3 TGA-DTG Thermogram of PEGDAF.

Sulfonation eugenol diallyl phthalate copolymer (SPEGDAF)

The sulfonation process of PEGDAF was carried out with a sulfuric acid sulfonation agent. The addition of sulfonate groups was carried out to increase the electrical conductivity of PEGDAF. The sulfonation reaction of PEGDAF is shown in **Figure 4**. SPEGDAF is a blackish brown solid which is soluble in methanol, ethyl acetate, chloroform, dichloromethane and insoluble in distilled water. The melting point and molecular weight obtained increased from 84 - 110 °C and from 7,611.06 daltons - 1,3674.54 daltons. This occurs because the addition of sulfonate groups ($–SO_3H$) causes an increase in molecular weight.

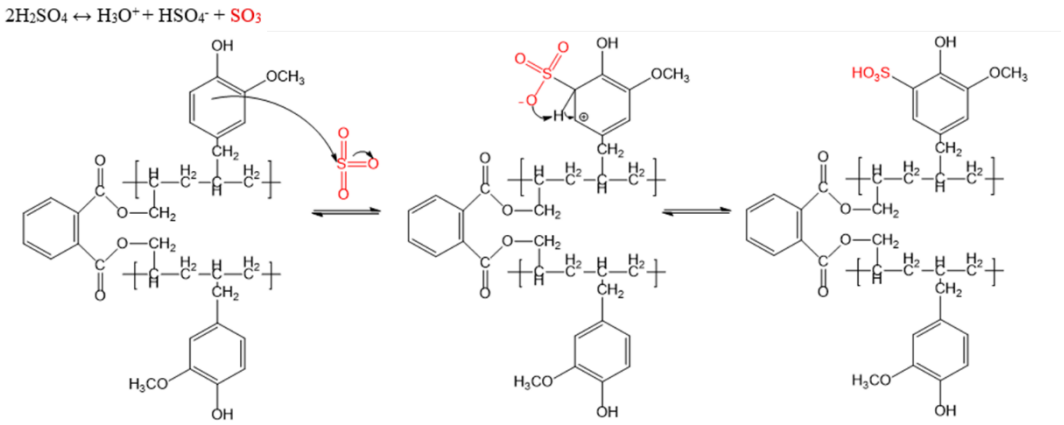

Figure 4 Sulfonation Reaction of PEGDAF.

Determination of cation exchange capacity (CEC) is carried out using the acid-base titration method. SPEGDAF is soaked in NaOH solution, which will substitute the sulfonate group ($–SO_3H$), namely Na^+ ions substitute H^+ ions to produce H_2O and leave unreacted NaOH. The reaction between ($–SO_3H$) and NaOH shown in **Figure 5**. NaOH that has not reacted with ($–SO_3H$) is able to determine the CEC in SPEGDAF [13]. CEC functions to test the ability of a polymer to provide cations contained in its functional groups with cations in the system. The easier it is for a compound to release H^+ ions, the greater its cation exchange capacity. In supercapacitors, polymers must have a large CEC so that they can increase the polymer's ability to conduct electricity [23]. Determination of the average amount of ($–SO_3H$) in each polymer chain unit is measured by determining the degree of sulfonation (DS). A higher CEC corresponds to a higher DS in sulfonated copolymers.

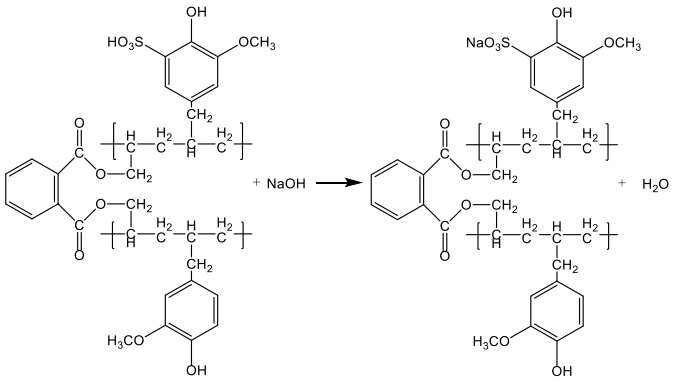

Figure 5 Substitution Reaction on Determining CEC and DS.

The cation exchange capacity (CEC) value in SPEGDAF is calculated using Eq. (1)

$$\text{CEC} = \frac{(V_{Blank} - V_{Sample}) \times M_{NaOH}}{Sample\ Weight} \quad (1)$$

The degree of sulfonation (DS) value in SPEGDAF is calculated using Eq. (2)

$$DS = CEC \times 10^{-3} \times \text{Mol.wt } SO_3H \times 100\% \quad (2)$$

where, V_{blank} refers to volume of the NaOH solution, V_{sample} represents the volume of the sample containing the NaOH solution, and M_{NaOH} is the molarity of the NaOH solution.

The calculation results of CEC and DS of SPEGDAF were obtained at 3.856 meq/g and 31.16%. The success of sulfonation in SPEGDAF can be seen through its DS value. Polymers that have a degree of sulfonation of more than 40% can easily dissolve in water.

The formation of sulfonate groups (−SO_3H) in SPEGDAF can be analyzed using FTIR as shown in **Figure 6**. Absorption band of the sulfonate groups S=O, S−O, and C−S appear. Comparison of FTIR absorption data of PEGDAF and SPEGDAF is shown in **Table 1**. Based on data obtained, S=O and C−O ether groups had the same wave number (1,213 cm^{-1}). This occurs because of the accumulation of peaks between the S=O and C−O ether groups. Therefore, deconvolution of the FTIR spectra was carried out to prove the presence of S=O as shown in **Figure 7**. The deconvolution showed the addition of derivative peaks, namely two absorptions, C−O ether (1,213 cm^{-1}) and S=O (1,227 cm^{-1}) while PEGDAF has C−O ether absorption (1,216 cm^{-1}). The presence of S=O groups in sulfonated eugenol diallyl phthalate copolymers in the FTIR spectra deconvolution proves that sulfonation was successful.

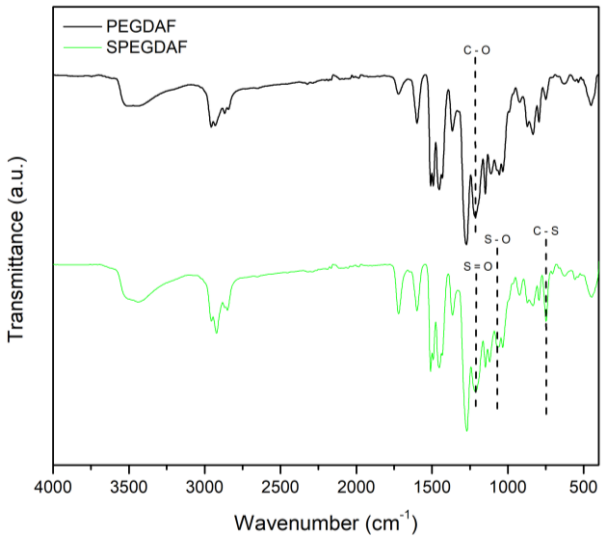

Figure 6 FTIR Spectra of SPEGDAF.

Table 1 Absorption ranges of PEGDAF before and after sulfonation.

Functional group	Wavenumber (cm^{-1})	
	PEGDAF	SPEGDAF
C−O stretching	1,216	1,213
S=O stretching	-	1,213
S−O stretching	-	1,059
C−S stretching	-	748

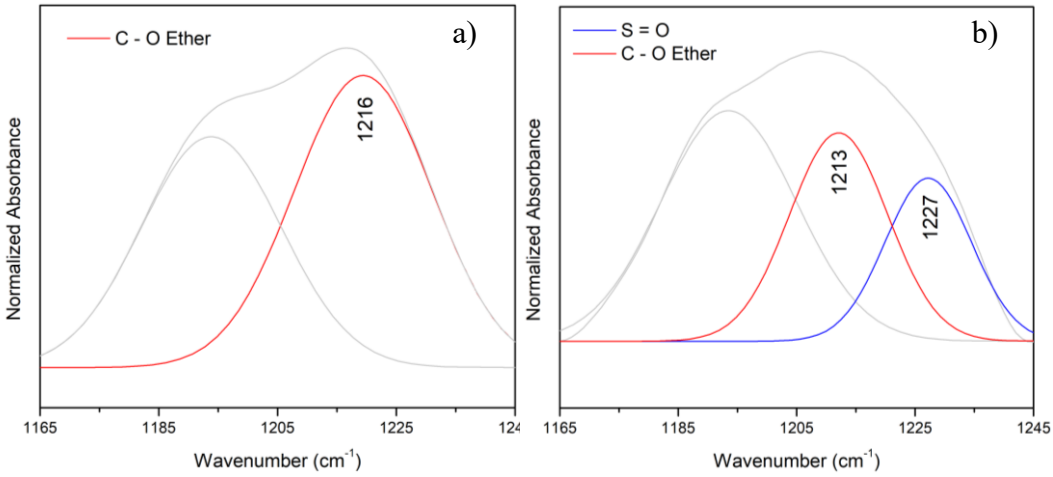

Figure 7 Deconvolution of FTIR spectrum of a) PEGDAF and b) SPEGDAF.

The thermal resistance of SPEGDAF was measured by TGA-DTG analysis as shown in **Figure 8**. The mass reduction of 5% and 10% in SPEGDAF occurred at temperatures of 169 and 215 °C, which were lower than PEGDAF. The decrease in the thermal resistance of SPEGDAF was due to the degradation of sulfonate groups [17]. The presence of sulfonate groups tends to increase polarity and decrease its thermal stability, so that sulfonated polymers tend to degrade at lower temperatures [24].

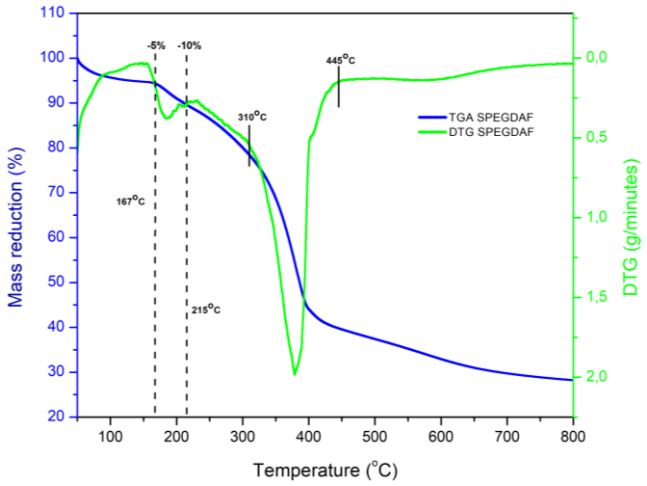

Figure 8 TGA-DTG Thermogram of SPEGDAF.

Synthesis of graphene oxide (GO)

Graphene oxide (GO) was synthesized using a modified hummer method, which does not use $NaNO_3$ which can produce toxic gases NO_2 and N_2O_4 [25]. This method runs through two stages, namely the oxidation and exfoliation processes that shown in the **Figure 9**. The reaction of $KMnO_4$ with graphite will form a graphite oxidation process due to the release of oxygen atoms from decomposition of $KMnO_4$. Hydrogen peroxide (H_2O_2) is added to quench the oxidation reaction and to reduce any remaining potassium permanganate ($KMnO_4$), ensuring the completion of the reaction [26]. The next step involves exfoliation using the ultrasonication method to separate the layers of graphite oxide. The ultrasonic waves disrupt the van der Waals forces between the layers, resulting in the formation of graphene oxide sheets [27].

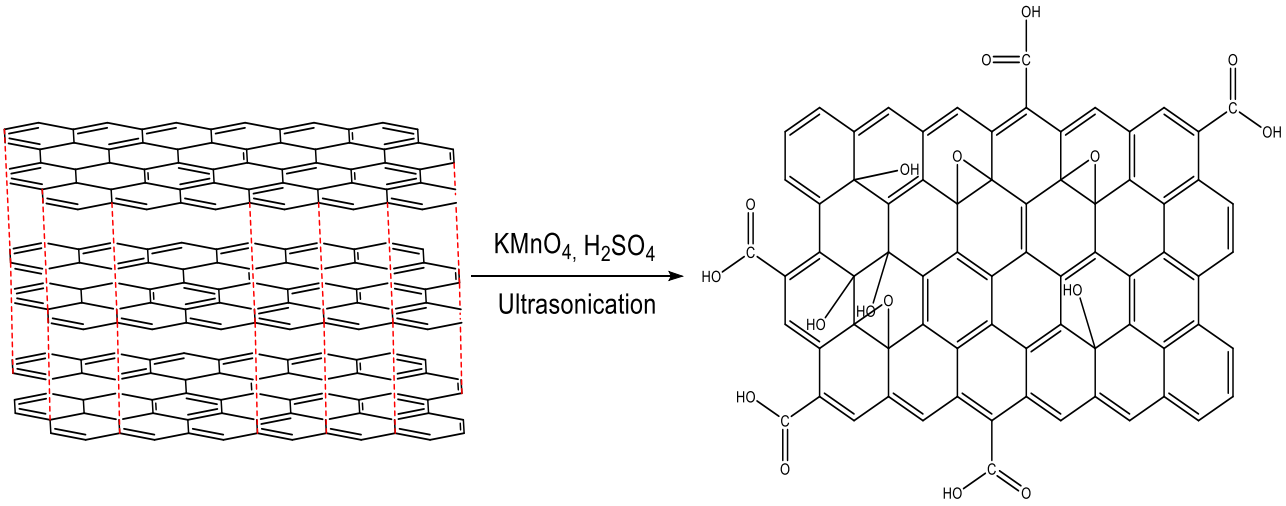

Figure 9 Ilustration of Synthesis GO.

The synthesized GO are brownish black sheets with a yield of 62.5%. The resulting color is a form of light absorption by the stacking of graphene oxide sheets. The oxygen functional groups in GO were analyzed using FTIR as shown in **Figure 10**. The absence of significant peaks in graphite indicates the inert chemical nature of graphite and its very stable and symmetrical bond structure [28]. The absorption bands of GO oxygen groups were obtained, O−H (3338 cm^{-1} and 1,407 cm^{-1}), C=O stretching (1,717 cm^{-1}) and C−OH stretching (1,227 cm^{-1}) indicating the presence of −COOH groups. In addition, absorption wave numbers C=C (1,622 cm^{-1}) and C−O (1,051 cm^{-1}) appeared which indicated the presence of C−O−C groups.

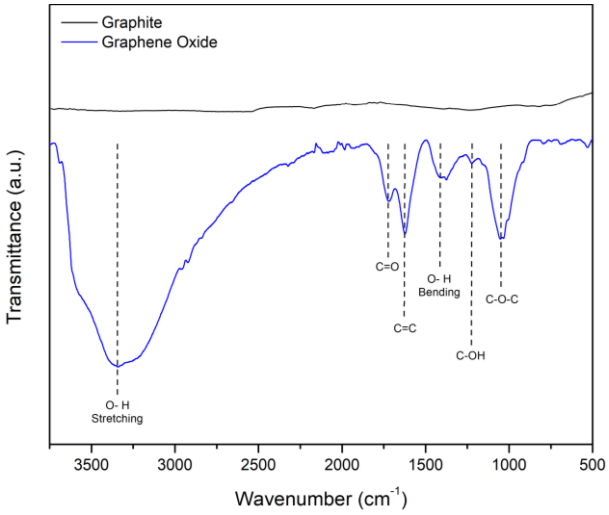

Figure 10 FTIR Spectra of Graphene Oxide.

The success of the synthesis is also shown by comparing the results of the XRD analysis between GO and graphite. The X-ray diffraction pattern obtained at the diffraction angle of 2θ in the range of 5° - 90° is used to identify the d-spacing and the crystal size of GO. The results of the XRD analysis are shown in **Figure 11**.

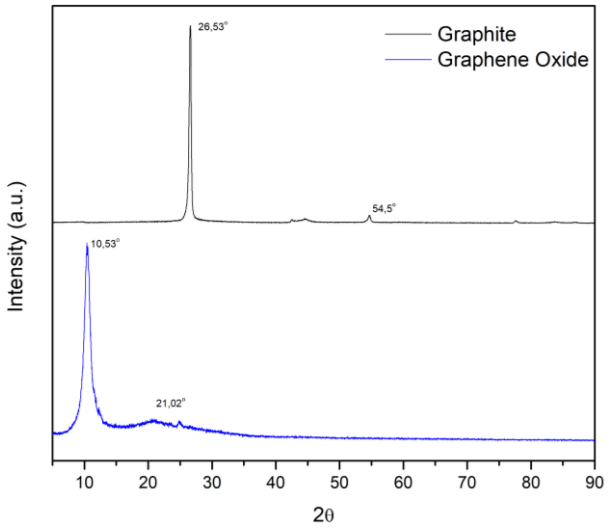

Figure 11 XRD Patterns of Graphene Oxide.

The d-spacing corresponding to the most intense crystalline peaks of various samples was determined using Bragg's equation [29]:

$$n\lambda = 2d\sin\theta \quad (3)$$

Where n represents an integer value (with n = 1), λ denotes the wavelength of the X-ray source (CuKα$_1$ = 1.54 Å), and θ is the angle formed between the incident and reflected rays.

The crystallite size (D) corresponding to the most intense crystalline peak is determined through the Debye-Scherrer equation [30].

$$D = \frac{K\lambda}{\beta_s \cos\theta} \quad (4)$$

Where K = 0.89 is the shape factor associated with the average crystallite size, λ is the wavelength of CuKα radiation and is 0.154 nm, θ is Bragg's angle of diffraction, and β_s refers to the full width at half maximum (FWHM) of the crystalline peak, expressed in radians.

The calculation results are shown in **Table 2**. The shift in the diffraction peak occurs due to the presence of oxygen functional groups from the oxidation process. The crystal size of GO shows the resulting d-spacing, the smaller the crystal size produced, greater the d-spacing due to the increased formation of oxygen functional groups in the interlayer [31]. A smaller crystal size will form a low intensity related to high oxidation in GO [32].

Table 2 The Interlayer Spacing's (d) and Crystallite Size (D) of The Materials.

Samples	2θ (º)	θ (º)	d (Å)	D (nm)
Graphite	26.53	13.265	3.35	24.63
Graphene Oxide	10.53	5.265	8.39	7.06

Synthesis of sulfonated eugenol diallyl phthalate copolymer/graphene oxide composite (SPEGDAF/GO)

SPEGDAF/GO composite was synthesized through physical dispersion method with stirring and sonication. SPEGDAF and GO were mixed in tetrahydrofuran (THF) solvent to obtain a brownish black composite. The interaction between SPEGDAF and GO involves several different interaction mechanisms. The oxygen group (-OH) in the GO structure forms hydrogen bonds with the hydroxyl group in SPEGDAF. The phi-phi interaction is also formed due to the interaction between the benzene rings of the material, creating a connection between the two materials but does not produce a new functional group. The proposed interaction between SPEGDAF and GO is shown in **Figure 12**.

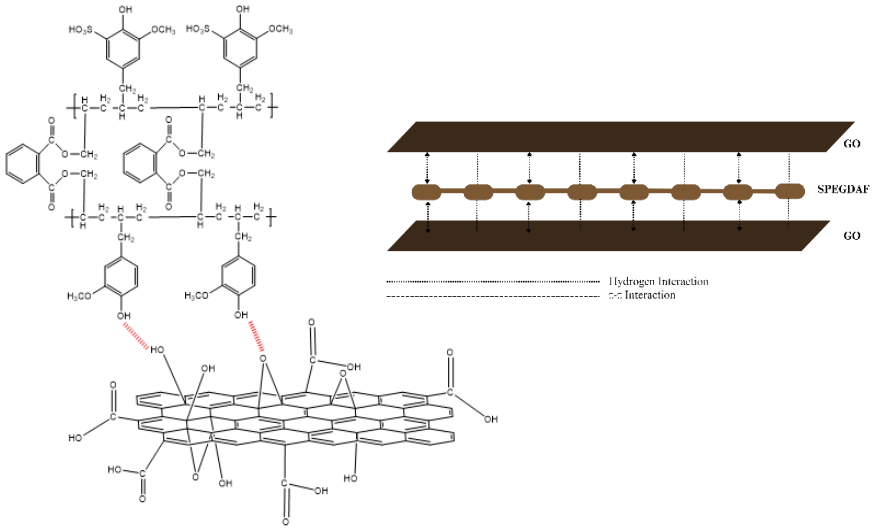

Figure 12 Proposed Interaction of SPEGDAF/GO Composite.

FTIR was performed to determine the functional groups in the SPEGDAF/GO composite as shown in **Figure 13**. It shows the absorption peaks of C=O (1,721 cm^{-1}), aromatic C=C (1,600 cm^{-1}), S=O (1,213 cm^{-1}), S−O (1,057 cm^{-1}), and C−S (748 cm^{-1}). The wider O−H group absorption peak in the composite compared to SPEGDAF indicates the presence of more hydrogen groups due to the presence of graphene oxide. The typical peak of graphene oxide in the composite is difficult to see due to the overlapping absorption peaks between GO and SPEGDAF.

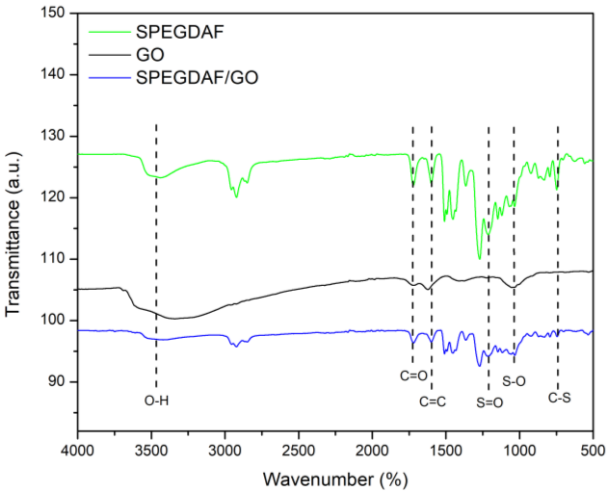

Figure 13 FTIR Spectra of SPEGDAF/GO Composite.

Electrochemical performance

The specific capacitance (C_{sp}) of the electrode was tested using cyclic voltammetry with 1 M HCl electrolyte solution and at scan rate of 5 mV/s. The voltammogram showed pseudocapacitive properties because there was a redox peak resulting from the faradic reaction. The surface area of the SPEGDAF/GO composite voltammogram results was larger than SPEGDAF and PEGDAF. The larger the surface area of a material in the cyclic voltammogram, the greater its ability to absorb and release charges maximally [21]. This is able to increase the specific capacitance of the supercapacitor electrode to store a larger charge. These results are shown in the graph of the specific capacitance of PEGDAF, SPEGDAF, and SPEGDAF/GO in **Figure 14**.

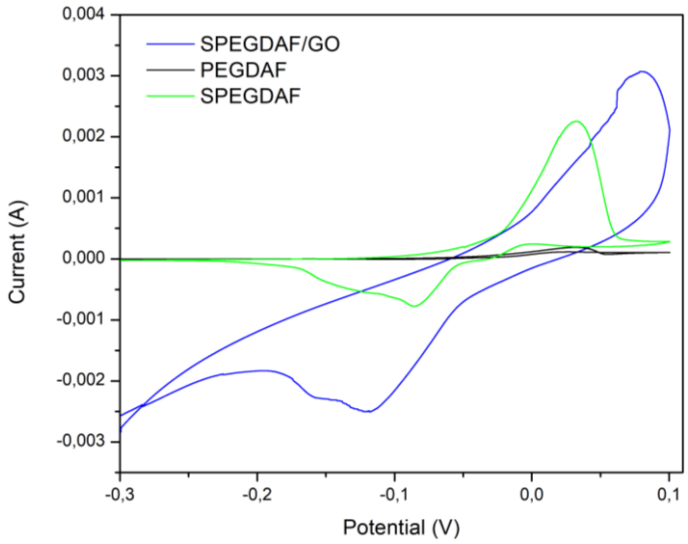

Figure 14 CV Voltammogram of PEGDAF, SPEGDAF, and SPEGDAF/GO.

The specific capacitance is calculated using Eq. (6) [33].

$$C_{sp} = \frac{1}{m \times k \times (V_1 - V_2)} \int Iv.dv \quad (6)$$

Where, $(V_1 – V_2)$ the working potential window (0.4 V), m refers to the mass of the active electrode material (g), k is the scan rate (mV/s), and $\int I_v\, dv$ represents the area under the current voltage curve covered by the active material.

Based on the calculations and graphs, the specific capacitance of PEGDAF, SPEGDAF, and SPEGDAF/GO is 0.026, 0.79 and 2.47 F/g. The higher specific capacitance of SPEGDAF compared to PEGDAF correlates with its greater cation exchange capacity. A higher cation exchange capacity enhances ionic mobility and charge storage, thereby increasing the polymer's overall electrical conductivity [34]. The specific capacitance of the composite is the largest because GO has a large specific surface area (around 2,391 m^2/g) making the contact area with the electrolyte larger and increasing the specific capacitance [35]. The specific capacitance value of a supercapacitor electrode material is around 5.844×10^{-9} up to 2,700 F/g [36]. Based on the results obtained, it is proven that the SPEGDAF/GO composite material has great potential as an environmentally friendly material for supercapacitor electrodes and this also shows that the compositing of SPEGDAF with GO can increase the specific capacitance of the supercapacitor electrode.

The electrical conductivity of the electrode was tested using Electrochemical Impedance Spectroscopy (EIS) with 1 M HCl electrolyte solution and a frequency range of 0.01 Hz-10^5 Hz. Based on EIS obtained, the electrolyte resistance (Rs) and charge transfer resistance (Rct) values of PEGDAF, SPEGDAF, and SPEGDAF/GO are shown in **Table 3**.

Table 3 The electrolyte resistance (Rs) and charge transfer resistance (Rct) values of working electrode.

Samples	Rs (ohm)	Rct (ohm)
PEGDAF	4.86	51.27
SPEGDAF	3.42	45.16
SPEGDAF/GO	3.02	29.87

The Rs and Rct values of SPEGDAF are lower than PEGDAF because the sulfonate group in SPEGDAF makes ion transfer faster between electrolyte and electrode. In the SPEGDAF/GO composite, both Rs and Rct values are lower compared to SPEGDAF alone, as the layered or sheet-like structure of GO facilitates rapid ion transport, resulting in reduced resistance. The lower the Rs and Rct values, the greater the ion

conductivity value during charging and discharging [37]. These results are supported by the Nyquist plot of PEGDAF, SPEGDAF, and SPEGDAF/GO in **Figure 15**.

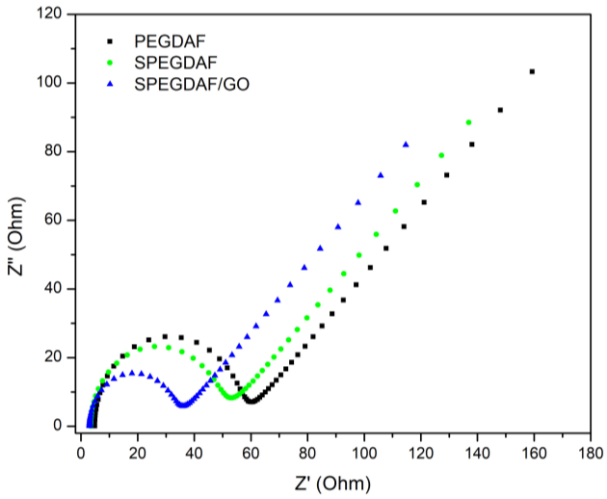

Figure 15 Nyquist plots of PEGDAF, SPEGDAF, and SPEGDAF/GO.

The specific capacitance is calculated using Eq. (7) [38].

$$\sigma = \frac{I}{R_b \times A} \quad (7)$$

Where, R_b is bulk resistance measured (Ω), while I refers to the thickness of the electrode (cm), and A represents the surface area of the electrode (cm^2).

Based on the calculations and graphs obtained, the electrical conductivity of PEGDAF, SPEGDAF, and SPEGDAF/GO is 2.34×10^{-4}, 2.65×10^{-4} and 4.02×10^{-4} S/cm. The conductivity value of a material to be classified as a semiconductor is around 10^{-8} - 10^{3} S/cm [25]. Based on the results obtained, it is proven that the SPEGDAF/GO Composite material has great potential as an environmentally friendly material for supercapacitor electrodes and this also shows that the compositing of SPEGDAF with GO can increase the electrical conductivity of supercapacitor electrodes.

Conclusions

This study successfully synthesized SPEGDAF/GO composites through physical mixing of sulfonated eugenol diallyl phthalate copolymer and graphene oxide with a mass ratio of 9:1. The synthesis of PEGDAF and its sulfonation process were proven successful through FTIR, TGA analysis, and characterization of melting point and molecular weight. Sulfonation increased the cation exchange capacity to 3.856 meq/g and produced a sulfonation degree of 31.16%. Graphene oxide synthesized using the modified Hummers method showed success through the emergence of oxygen groups (–OH, –COOH, –CHO, epoxy) and typical diffraction peaks on XRD. The SPEGDAF/GO composite showed improved supercapacitor electrode performance, with a specific capacitance of 2.47 F/g and an electrical conductivity of 4.02×10^{-4} S/cm. These results indicate that the composite has the potential to be an environmentally friendly and functional supercapacitor electrode material.

Acknowledgements

The authors gratefully acknowledge the financial support provided by Diponegoro University via international publication research scheme (RPI) Based on Agreement/Contract Number: 222-496/UN7.D2/PP/IV/2025.

Declaration of generative AI in scientific writing

The authors utilized ChatGPT-4.0 during the preparation of the manuscript to help enhance the clarity and quality of the language.

CRediT author statement

Ngadiwiyana Ngadiwiyana: Supervision, Conceptualization, Resources, Data curation, Formal

analysis, Funding Acquisition and Writing – review & editing. **Andi Nugroho**: Supervision, Data curation, Resources, and Writing – original draft. **Ismiyarto Ismiyarto**: Resources, Formal analysis, Supervision. **Purbowatiningrum Ria Sarjono**: Resources, Formal analysis, Supervision. **Damar Nurwahyu Bima**: Data curation, Supervision, Writing – original draft. **Irma Fifa Yanti**: Data curation, Writing – original draft.

References

[1] YM Volfkovich. Electrochemical supercapacitors (a review). *Russian Journal of Electrochemistry* 2021; **57(4)**, 311-347.

[2] AG Olabi, Q Abbas, AA Makky and MA Abdelkareem. Supercapacitors as next generation energy storage devices: Properties and applications. *Energy* 2022; **248**, 123617.

[3] P Lamba, P Singh, P Singh, P Singh, Bharti, A Kumar, M Gupta and Y Kumar. Recent advancements in supercapacitors based on different electrode materials: Classifications, synthesis methods and comparative performance. *Journal of Energy Storage* 2022; **48**, 103871.

[4] G Sumdani, MR Islam, ANA Yahaya and S Safie. Recent advancements in synthesis, properties, and applications of conductive polymers for electrochemical energy storage devices: A review. *Polymer Engineering & Science* 2021; **62(2)**, 269-303.

[5] RA Sheldon. Green carbon and the chemical industry of the future. *Philosophical Transactions of the Royal Society A* 2024; **382(2282)**, 20230259.

[6] NBA Prasetya, MR Putri, Ngadiwiyana and Gunawan. Polyeugenol-gum arabic/graphene oxide composite coating for high performance anticorrosion material. *Case Studies in Chemical and Environmental Engineering* 2024; **9**, 100658.

[7] VJV Vinayak, K Deshmukh, VRK Murthy and SKK Pasha. Conducting polymer based nanocomposites for supercapacitor applications: A review of recent advances, challenges and future prospects. *Journal of Energy Storage* 2024; **100**, 113551.

[8] Z Zhai, X Du, Y Long and H Zheng. Biodegradable polymeric materials for flexible and degradable electronics. *Frontiers in Electronics* 2022; **3**, 985681.

[9] Ngadiwiyana, Gunawan, NBA Prasetya, TD Kusworo and H Susanto. Synthesis and characterization of sulfonated poly (eugenol-co-allyleugenol) membranes for proton exchange membrane fuel cells. *Heliyon* 2022; **8(12)**, 12401.

[10] A Kausar. Poly (ether ether ketone) nanocomposites with graphene and derivative nanoreinforcements - contemporary scientific paragon and prospering breakthroughs. *Polymer-Plastics Technology and Materials* 2025; **64(7)**, 973-997.

[11] A Darmawan, AFN Sabarina, DN Bima, H Muhtar, CW Kartikowati and TE Saraswati. New design of graphene oxide on macroporous nylon assisted polyvinyl alcohol with Zn (II) cross-linker for pervaporation desalination. *Chemical Engineering Research and Design* 2023; **195**, 54-64.

[12] A Darmawan, H Muhtar, DN Pratiwi, DN Bima, C Panatarani, NL Hamidah and EC Prima. Thin-Film Nanofiltration membrane of polyaniline Decorated graphene oxide via In-Situ polymerization for ion separation. *Separation and Purification Technology* 2025; **356**, 129975.

[13] S Singh, TSSK Naik, N Shehata, L Aguilar-Marcelino, K Dhokne, S Lonare, V Chauhan, A Kumar, J Singh, PC Ramamurthy, AH Khan, NA Khan and MH Dehghani. Novel insights into graphene oxide-based adsorbents for remediation of hazardous pollutants from aqueous solutions: A comprehensive review. *Journal of Molecular Liquids* 2023; **369**, 120821.

[14] S Tamang, S Rai, R Bhujel, NK Bhattacharyya, BP Swain and J Biswas. A concise review on GO, rGO and metal oxide/rGO composites: Fabrication and their supercapacitor and catalytic applications. *Journal of Alloys and Compounds* 2023; **947**, 169588.

[15] H Chaudhuri and Y-S Yun. A critical review on the properties and energy storage applications of graphene oxide/layered double hydroxides and

graphene oxide/MXenes. *Journal of Power Sources* 2023; **564**, 232870.

[16] R Kumar and R Thangappan. Electrode material based on reduced graphene oxide (rGO)/transition metal oxide composites for supercapacitor applications: A review. *Emergent Materials* 2022; **5**, 1881-1897.

[17] Ngadiwiyana, CN Nabila, Ismiyarto and M Christwardana. Sulfonation of eugenol-diallyl phthalate copolymer as base material of supercapacitor electrode material *Jurnal Kimia Sains dan Aplikasi* 2024; **27(11)**, 523-530.

[18] B Li, W Tang, D Sun, B Li, Y Ge, X Ye and W Fang. Electrochemical manufacture of graphene oxide/polyaniline conductive membrane for antibacterial application and electrically enhanced water permeability. *Journal of Membrane Science* 2021; **640**, 119844.

[19] E Kianfar. Advances in nanoelectronics: Carbon nanotubes, graphene, and smart polymers: A review. *Trends in Sciences* 2025; **22(7)**, 9843.

[20] S Rattanaveeranon and K Jiamwattanapong. Enhancing supercapacitor performance with multilayered tungsten (VI) Oxide Nanoparticles/Reduced graphene oxide and activated carbon. *Trends in Sciences* 2025; **22(9)**, 10377.

[21] Ngadiwiyana, NBA Prasetya, Gunawan, TD Kusworo and H Susanto. Synthesis, characterization, and study of proton exchange polymer membrane properties of sulfonated copolymer eugenol-diallyl Phthalate. *Indonesian Journal of Chemistry* 2021; **21(1)**, 168-178.

[22] N Mendez-Lozano, F Peerez-Reynoso and C Gonzaalez-Gutieerrez. Eco-friendly approach for graphene oxide synthesis by Modified Hummers method. *Materials* 2022; **15(20)**, 7228.

[23] S Suriyakumar, P Bhardwaj, AN Grace and AM Stephan. Role of polymers in enhancing the performance of electrochemical supercapacitors: A review. *Batteries & Supercaps* 2021; **4(4)**, 571-584.

[24] L Francisco-Vieira, R Benavides, LD Silva, E Cuara-Diaz and D Morales-Acosta. Effect of sulfonating agent in the properties of styrene copolymers for PEMFC membranes. *International Journal of Hydrogen Energy* 2022; **47(70)**, 30303-30314.

[25] S Yadav, APS Raman, H Meena, AG Goswami, Bhawna, V Kumar, P Jain, G Kumar, M Sagar, DK Rana, I Bahadur and P Singh. An update on graphene oxide: Applications and toxicity. *ACS omega* 2022; **7(40)**, 35387-35445.

[26] Y Wang, K Zheng, H Guo, L Tian, Y He, X Wang, T Zhu, P Sun and Y Liu. Potassium permanganate-based advanced oxidation processes for wastewater decontamination and sludge treatment: A review. *Chemical Engineering Journal* 2023; **452**, 139529.

[27] MG Sumdani, MR Islam, ANA Yahaya and SI Safie. Recent advances of the graphite exfoliation processes and structural modification of graphene: A review. *Journal of Nanoparticle Research* 2021; **23**, 253.

[28] S Ghosh, A Kuttasseri, S Akhila, S Khamaru, NPB Aetukuri, A Mahata and SK Martha. Understanding critical bottlenecks of anion intercalation into graphite: Operando gas evolution, host fluorination, site blocking, and structural issues. *Chemical Engineering Journal* 2025; **519**, 164880.

[29] S Bhadr and D Khastgir. Determination of crystal structure of polyaniline and substituted polyanilines through powder X-ray diffraction analysis. *Polymer Testing* 2008; **27(7)**, 851-857.

[30] N Tohluebaji, N Muensit, C Putson, GA Ashraf, P Channuie, P Porrawatkul, U Wanthong and J Yuennan. Multi-functional enhancement of P(VDF-HFP) nanocomposites through MWCNTs loading for piezoelectric sensing. *Journal of Materials Research and Technology* 2025; **36**, 8475-8491.

[31] RS Rajaura, S Srivastava, V Sharma, PK Sharma, C Lal, M Singh, HS Palsania and YK Vijay. Role of interlayer spacing and functional group on the hydrogen storage properties of graphene oxide and reduced graphene oxide. *International Journal of Hydrogen Energy* 2016; **41(22)**, 9454-9461.

[32] L Shen, L Zhang, K Wang, L Miao, Q Lan, K Jiang, H Lu, M Li, Y Li, B Shen and W Zheng. Analysis of oxidation degree of graphite oxide and chemical structure of corresponding reduced

graphite oxide by selecting different-sized original graphite. *RSC advances* 2018; **8(31)**, 17209-17217.

[33] SR Yekkaluri, S Konda, D Velpula, RK Thida, SC Chidurala, BN Tumma, NR Nama and R Deshmukh. Comparative analysis of ZnO nanoparticle's specific capacitance in supercapacitors: The role of surfactant and stabilizing agent. *Applied Surface Science Advances* 2022; **12**, 100326.

[34] H Yang and N Wu. Ionic conductivity and ion transport mechanisms of solid-state lithium-ion battery electrolytes: A review. *Energy Science & Engineering* 2022; **10(5)**, 1567-1789.

[35] TKN Tran, HL Ho, HV Nguyen, BT Tran, TT Nguyen, PQT Bui and LG Bach. Photocatalytic degradation of Rhodamine B in aqueous phase by bimetallic metal-organic framework M/Fe-MOF (M= Co, Cu, and Mg). *Open Chemistry* 2022; **20(1)**, 52-60.

[36] A SI, GZ Kyzas, K Pal and FG de Souza Jr. Graphene functionalized hybrid nanomaterials for industrial-scale applications: A systematic review. *Journal of Molecular Structure* 2021; **1239**, 130518.

[37] AA Nada, AO Siskova, A Kleinova, AE Andicsova, Erik Simon and J Mosnacek. Ionic conductive cellulose-based hydrogels for Al-air batteries: Influence of the charged-functional groups on the electrochemical properties. *Journal of Power Sources* 2023; **572**, 233089.

[38] J Yuennan, N Muensit, N Tohluebaji, W Chailad, L Yang, N Sukhawipat, GA Ashraf and P Channuie. Tailoring dielectric properties and crystallinity in poly(vinylidene fluoride-co-hexafluoropropylene) nanocomposites via iron (III) chloride hexahydrate incorporation. *Scientific Reports* 2025; **15**, 17810.